RESEARCH ARTICLE

Editorial Process: Submission:10/25/2024 Acceptance:03/17/2025

Development and Characterization of Curcumin Loaded PEGylated Niosomal Nanoparticles: Potential Anti-Cancer Effect on Breast Cancer Cells through RFC Gene Expression

Neda Iranpoor[1,2], Davoud Jafari-Gharabaghlou[3], Siham Abdulzehra[3], Mohammad Reza Dashti[3], Fatemeh Ghorbanzadeh[3], Nosratollah Zarghami[3,4]*

Abstract

Background: Breast cancer is the second leading cause of cancer deaths among women. Recent studies emphasize the significant role of folate metabolic pathways in cancer progression. The Reduced Folate Carrier (*RFC*), a folate transporter in cell membranes, plays an essential role in transporting folate receptor-dependent drugs. Curcumin, a bioactive compound with anticancer and anti-inflammatory effects, is hindered by low stability and a short half-life. Niosomes are versatile nanoparticles that can deliver both hydrophilic and hydrophobic drugs. **Objective:** This study aims to evaluate the anticancer effects of curcumin-loaded niosomal nanoparticles, focusing on their impact on *RFC*, *BAX*, and *BCL-2* gene expression in MDA-MB-231 breast cancer cells. **Methods:** Curcumin-loaded noisomal nanoparticles were synthesized by the thin-film hydration method. Then, the morphology, size, and physico-chemical nanoparticles were determined by FE-SEM, DLS, and FT-IR methods, respectively. The MTT results determined the cytotoxicity of free and nano-formulated curcumin; also, the gene expression of *RFC*, *BCL-2*, and *BAX* was evaluated using the Real-Time PCR method. Furthermore, apoptosis and cell cycle analysis were investigated by Flow cytometry. **Results:** The results of the physicochemical characteristics of the nanoparticles showed that curcumin was appropriately loaded in niosomal NPs. The MTT results showed that curcumin loaded in niosomal NPs has a higher anti-proliferative effect than free curcumin. Real-time PCR results showed increased *RFC* and *BAX* gene expression and decreased *BCL-2* gene expression; this change was more significant in the treatment with nano-formulated curcumin. The apoptosis and cell cycle analysis also confirmed that free and nano-formulated curcumin induces apoptosis and cell cycle arrest. **Conclusion:** Overall, the results suggested that curcumin loaded in niosomal nanoparticles effectively improves the anticancer effect and could be a capable approach for treating breast cancer.

Keywords: Curcumin- Breast cancer- Niosome nanoparticles- Reduced folate carrier

Asian Pac J Cancer Prev, **26 (3)**, 1017-1026

Introduction

Breast cancer is one of the most causes of cancer death among women, and its prevalence has surpassed lung cancer in recent years. Breast cancer is commonly treated with chemotherapy, but it has limitations such as high toxicity, drug resistance, and high cost [1, 2]. To improve breast cancer therapy, alternative treatments such as combination chemotherapy and intervention of bioactive compounds have been developed [3-5]. Bioactive compounds are natural agents called phytochemicals that have biological activity and nutritional value. In recent years, studies clearly show which diets include fruits, vegetables, and fibers (foods of plant origin) to prevent dangerous diseases (heart diseases, obesity, diabetes, and cancer) or reduce their risks. These compounds reduce the side effects of chemotherapy drugs [6-9]. One such bioactive compound is curcumin, which has shown to have anticancer effects. It has been shown to inhibit various molecular pathways involved in cancer development, including the NF-κB and COX-2 pathways. Curcumin not only blocks transcription and expresses 2 (COX-2) but also modulates S-glutathione transferase activity, which influences early carcinogenesis and may reduce cancer cell resistance to chemotherapy (Bengmark, 2006). However, curcumin has low solubility and absorption, so encapsulating it in nanoparticles can enhance its effectiveness [10]. This substance is stable in physiological

*[1]Zanjan Metabolic Diseases Research Center, Zanjan University of Medical Sciences, Zanjan, Iran. [2]Biochemistry Department, Zanjan university of medical sciences, Zanjan, Iran. [3]Department of Clinical Biochemistry and Laboratory Medicine, Faculty of Medicine, Tabriz, Iran. [4]Department of Medical Biochemistry, Faculty of Medicine, Istanbul Aydin University, Istanbul, Turkey. *For Correspondence: zarghami@tbzmed.ac.ir*

pH and acidic conditions, but it degrades quickly in basic environments (by over pH=8). Curcumin is a hydrophobic and insoluble molecule in water [11]. Curcumin prevents transcription and expression of cyclooxygenases 2 (COX 2) by blocking NF-κB pathway [12]. Also, this compound increases the expression of S-glutathione transferase activity in cells and hinders the early stages of carcinogenesis but these enzymes rise in advanced stages of cancer which cause cancer cell resistance to chemotherapy drugs. Due to the low solubility and high sensitivity of curcumin to physiological pH changes in the body as well as its low absorption through the gastrointestinal, encapsulating curcumin in nanoparticles can increase its effectiveness and toxicity for cancer cells (Figure 1) [13, 14]. Nanocarriers such as niosomes, which are lipid-based carriers, have been found to be effective in delivering drugs specifically to cancerous tissues. Niosomes have advantages such as biocompatibility, slow release, and the ability to encapsulate various types of drugs [15-20]. Niosome has the ability to entrapping different types of hydrophilic and hydrophobic drugs, proteins, genes and vaccines [16, 21, 22]. PEGylation of niosomes further improves their stability and drug encapsulation. Besides, it decreases the size of nanoparticles, drug release a long period of time, and also it provides an easy method for drug delivery system [23-25]. *RFC* (Reduced Folate Carrier) is a membrane antiport transporter that is present in most tissues which can carry antifolate drugs such as methotrexate (MTX) to the cell [26-28]. Long-term administration of high doses of MTX can causes various side effects such as liver, lung and kidney disorders [29]. Folate metabolism has been found to play a crucial role in cancer development, and disruption of this system can cause tumor growth. Anti-folate drugs, such as methotrexate, can be delivered to cancer cells through the Reduced Folate Carrier (*RFC*). However, high doses of methotrexate can cause side effects, so researchers are exploring nanotechnology-based drug delivery systems and combination therapies to reduce the dose and toxicity of chemotherapy drugs (Figure 2) [30]. *RFC* usually is located in brush-border membrane of small and colon intestine, hepatocytes, the retinal pigment epithelium and basolateral membrane of the renal tubular epithelium [31, 32].

B-cell Lymphoma 2 (*Bcl-2*) protein has an anti-apoptotic role and prevents cell death. *Bcl-2* is often over-expressed in cancer cells [33]. *Bcl-2* family members include BAK and *BAX* which are pro-apoptotic factors and cause the cytochrome c releasing and disruption of mitochondrial function and induction of apoptosis. In fact, *Bcl-2* and *BAX* have opposite actions [34]. *BAX* is regulated by p53-mediated apoptosis. The studies have shown that the p53 signaling pathway is involved in the transcriptional activation of *BAX* in apoptosis and also in changing the ratio of BCL-XL to *BAX*. It was also shown that curcumin induces cell apoptosis in a p53-dependent pathway and decreases BCL-XL by *BAX* as effective regulatory molecule [35]. In the current study, we synthesized and characterized curcumin-loaded-niosomal nanoparticles and evaluated their ant-cancer effect on MDA-MB-231 breast cancer cells through the *BAX*, *BCL-2*, and *RFC* genes expression. This method improves its bioavailability, stability, and ability to target cancer cells, overcoming the limitations of free curcumin. Furthermore, the study highlights the use of gene expression analysis (*BAX, BCL-2, RFC*) to assess the therapeutic efficacy, marking a significant advancement in targeted cancer therapy.

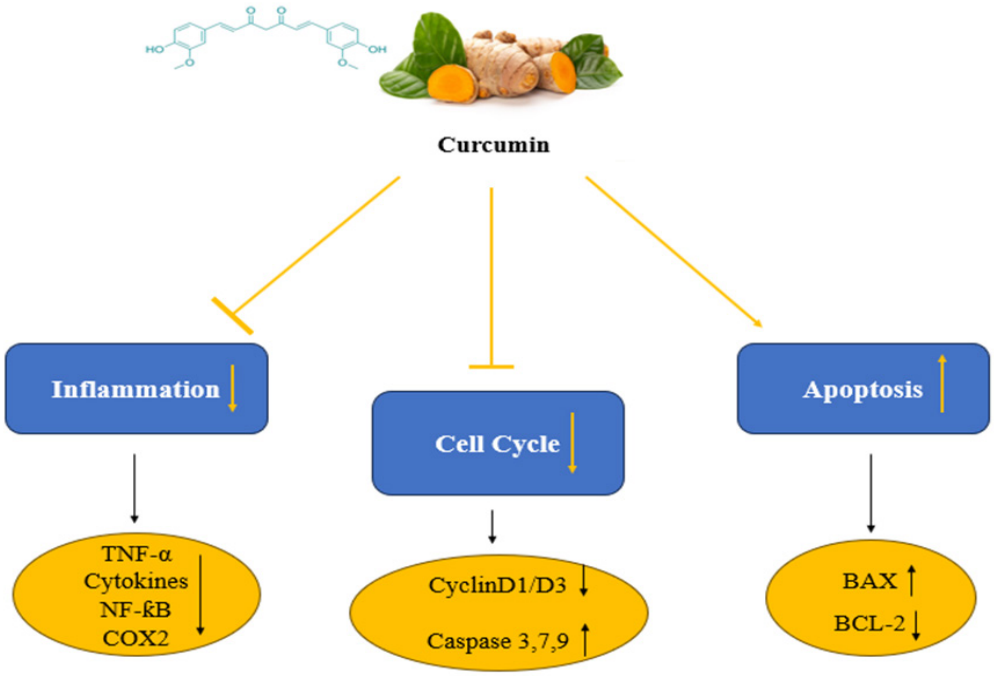

Figure 1. Mode of Action of Curcumin in Cancer. Curcumin, has an effect on reducing inflammation by inhibiting *TNF-a, COX2*, and NF-ƙB. By increasing caspases, it causes the cell cycle arrest. It also stimulates apoptosis of cancer cells by increasing *BAX* and decreasing *BCL-2* expression.

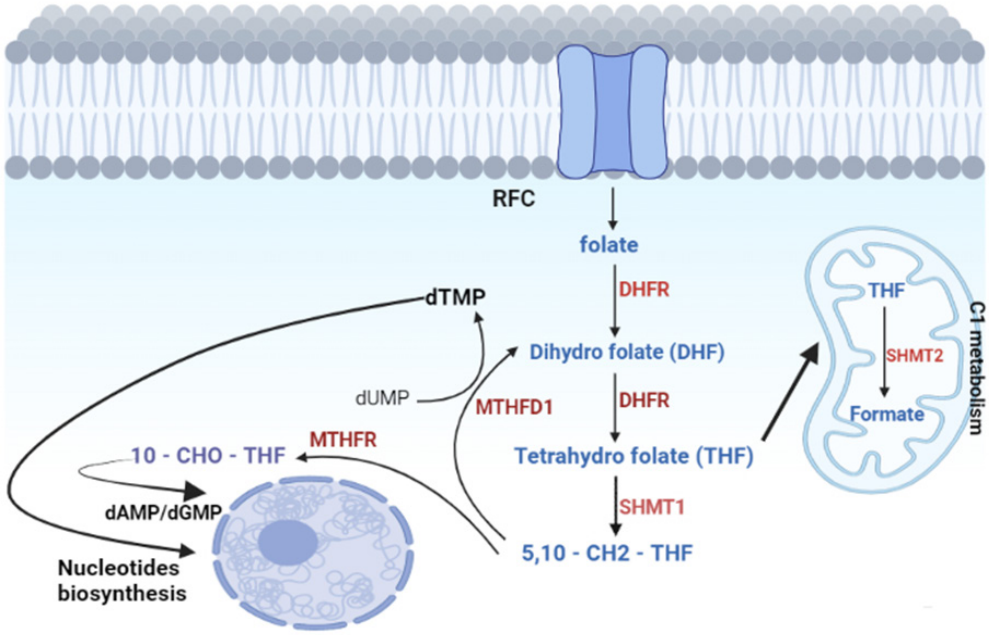

Figure 2. Metabolic Pathway of RFC. Reduced Folate enters the cell through the RFC carrier and is converted to DHF and THF by the DHFR enzyme. Then, THF proceeds in two ways. It was first converted to methylene THF with SHMT1, which is also very important in the production of DNA synthesis precursors. By MTHFR enzyme, methylene THF is converted into CHO – THF and DHF. In the second path, THF enters into the mitochondria where it is converted into Format by the enzyme SHMT2 this pathway is known as one-carbon metabolism. DHF: dihydrofolate; DHFR: dihydrofolate reductase; THF: tetrahydrofolate; MTHFR, methylenetetrahydrofolate reductase; SHMT1/2, serine hydroxymethyl transferase; MTHFD1, methylenetetrahydrofolate dehydrogenase 1.

Materials and Methods

Materials

MDA-MB-231 breast cancer cell line (Cat. No 10192) was obtained from the Cell Bank (Pasteur Institute, Iran). Curcumin (MW =368.38 g/mol), MTT powder, penicillin, streptomycin, polyethylene glycol (PEG, MW = 4000), and Dimethyl Sulfoxide (DMSO) were purchased from Sigma-Aldrich (St. Louis, MO, USA). RPMI-1640 and Fetal Bovine Serum (FBS) were prepared from Gibco (Invitrogen, UK). The cDNA synthesis kit was obtained from Fermentas (Vilnius, Lithuania), and the SYBR green PCR master mix and Trizol kit were bought from Roche (Germany).

Methods

Preparation of blank and Cur-loaded PEGylated niosome NPs

Nanoparticles were prepared using the thin film hydration method. In brief, cholesterol (0.0057 g), curcumin (0.0036g), span 60 (0.036g), and PEG (0.004g) were resolved in methanol (6ml) and chloroform (3ml) and were placed on a rotary evaporator (Heidolph Instruments, Hei-VAP series) under vacuum situation for 1 hour. Then, the solution was rested at room temperature for 45 minutes. Afterward, PBS (10ml) was added to the prepared emulsion and placed on the rotary again (1h). Then sonication was carried out with an ultrasonic probe for 20 min. In the sonication stage, the solution was rested for 2 minutes for every 1 minute of probe.

Characterization of Cur-loaded PEGylated niosome

The nanoparticle size, polydispersity index (PDI), and surface charge (zeta potential, mv) of free niosomal and cur-nio NPs were determined with Dynamic Light Scatting (DLS) (Malvern instrument, Malvern, UK). Then, in order to investigate the physicochemical properties of nanoparticles, samples were freeze-dried and assessed via the FT-IR technique. The surface morphology of the NPs was analyzed using a Field Emission Scanning Electron Microscope (FE-SEM) instrument, specifically the Hitachi S-4000 model. Additionally, Atomic Force Microscopy (AFM) from JPK Instruments AG in Berlin, Germany was utilized to examine the topography of the NPs.

Cell culture

Breast cancer cell line (MDA-MB-231) was cultured in RPMI-1640 (Gibco, USA) medium containing 10% FBS, penicillin/streptomycin, and 1% sodium bicarbonate. The cultured cells were incubated and grown in 5% CO_2 at 37˚C. These cells were controlled through an inverted microscope and passed after cell proliferation reached a density of 70 %.

Drug loading efficiency

After the synthesis of curcumin-loaded PEGylated niosome (Cur-nio), the encapsulation efficiency of Cur-nio NPs was investigated by separating the supernatant of the tube and assessment of non-entrapped drugs in UV-visible spectrophotometer device (PerkinElmer, CA, USA) with a wavelength of 425 nm of curcumin. Then, drug loading (DL) and entrapment efficiency (EE) of Cur-nio were calculated via the following formulas.

Table 1. The Designed Primers for *RFC, BCL-2*, and *BAX* Genes

Gene	Primer Sequence	PCR product
RFC	F: 5′- CCTTTTGGAGAATTGTGTCCT -3′	89
	R: 5′-AGACAGGCAAATAAAAGTGACC-3′	
Bcl-2	F: 5′-ACTTCTGCGAATACCGGACT-3′	148
	R: 5′-ATCCCAACCGGAGATCTCAAG-3′	
Bax	F: 5′-GGTTGTCGCCCTTTTCTA-3′	107
	R: 5′-CGGAGGAAGTCCAATGTC -3′	
β - actin	F: 5′- CAAGCAGGAGTATGACGAGT -3′	116
	R: 5′- GTTTTCTGCGCAAGTTAGGTT -3′	

$$DL\% = \frac{\text{Weight of drug loaded}}{\text{Weight of drug loaded NPs}} \times 100$$

$$EE\% = \frac{Weight\ of\ drug\ loaded}{Total\ weight\ of\ drug\ added} \times 100$$

Drug release pattern

For the drug release assessment, Cur-nio NPs (20-30 mg) were dispersed in PBS (5 ml) and put into the dialysis layer membrane (MW Cut off 3000) and set in PBS (20 ml) with 120 rpm blending at 37˚C. At the chosen time, the peripheral buffer was changed with fresh PBS, and the concentration of discharged curcumin in PBS was calculated by calibration curve at a wavelength of maximum absorbance (~ 425nm) and observation utilizing UV-visible spectroscopy (Perkin Elmer, CA, USA). The amount of drug release is evaluated in time intervals of 1-2 hours, 1-4 days, and even up to a week in physiological pH 7.4 (Healthy cells) and in acidic pH 5 (Cancer cells).

Cytotoxicity assay

To determine the cytotoxicity of Cur-nio and free Cur on MDA-MB-231 cells MTT (3-(4,5-dimethylthiazol-2-yl)-2,5-diphenyl tetrazolium bromide) assay was applied. MTT (Sigma, Germany) powder was dissolved in RPMI-1640 and PBS. Due to the sensitivity of the MTT solution to light, it was covered and placed in the refrigerator. MDA-MB-231 breast cancer cells were cultured into 96-wells plate (4×10^4 cells/well) and incubated for 24 h. Next, cells were treated with free Cur and Cur-nio at various concentrations (5, 10, 15, 20, 30, and 40μM). After 48h, an MTT solution was added to the wells and allowed to incubate for an additional 4 h. The contents of the wells were depleted and DMSO was added to the wells to determine the solubility of formazan. Finally, the absorbance was registered at 570 nm using an EL-800 Reader (Bio Tek, Winooski, VT).

Real-time PCR

RNA extraction and cDNA synthesis

Briefly, MDA-MB-231 cells were cultured in 6 wells plate (5×10^5 cells/well), then treated with free Cur and Cur-nio for 48h. For RNA extraction, 500 μL Trizol solution was to each well and kept at room temperature for 10 minutes, and the solution of the wells was transferred to 2 mL microtubes, and 200 μL chloroform was added and located in a centrifuge. Afterward, the upper layer created by every microtube, was picked up and transferred to another 6 microtubes, and cold isopropanol was added to them and centrifuged. In the end, DEPC water was added to them, and finally, the amount of extraction RNA was read via the Nanodrop (spectrophotometer, ND-1000) For cDNA synthesis, same volumes of RNA were taken from all samples and reverse transcribed by the first strand cDNA synthesis kit (Fermentase). Based on the cDNA (complementary DNA) synthesis kit protocol, 5μL of extracted RNA, 14μL of cDNA master mix, and 1μL of random hexamer primer were mixed, and then, these solutions were incubated according to manufacture protocol in the thermocycler instrument.

Real-Time PCR

Real-time PCR (reverse transcription polymerase chain reaction) is an efficient tool for quantitative determination of gene expression. The synthesized cDNA was amplified using quantitative real-time PCR with designed primers (Table 1). All of these probes allow the detection of PCR products by generating a fluorescent signal while the SYBR Green dye emits its fluorescent signal simply by binding to the double-stranded DNA in the solution. The RT-PCR profile was built up for 95 C for 10 min, taken after by 45 cycles of 95 C for 15 s, 58 C for 30 s, and 72 C for 60 s and softening 70–90. Finally, the relative expression of genes was normalized by the housekeeping gene (β- actin) and quantified by $2^{-\Delta\Delta Ct}$ method.

Apoptosis test

The apoptosis of cells was evaluated using flow cytometry and Annexin V/PI staining. MDA-MB-231 cells were seeded in a 6-well plate at a density of 2×10^5 cells/well and incubated at 37°C for 24 hours. The cells were then treated with IC_{50} concentrations of free cur and cur-nio. After 48 hours, the MDA-MB-231 cells were collected using trypsin, centrifuged, washed three times with PBS, and re-suspended in 90 μL of binding buffer. Subsequently, 5 μL of Annexin V-FITC and 5 μL of propidium iodide (PI) staining solutions were added, and the mixture was incubated for 20 minutes at room temperature in the dark. Following this, 400 μL of binding buffer was added to each tube and gently mixed. The apoptotic were then analyzed using flow cytometry (Biosciences, USA).

Cell cycle analysis

Cell cycle analysis was conducted through the assessment of DNA content using propidium iodide (PI) staining. Initially, a specific number of cells (2×105 cells/well) were seeded in a 6-well plate. Subsequently, these cells were exposed to IC_{50} concentrations of free curcumin and cur-nio, and incubated for 24 hours. After 48 hours, MDA-MB-231 cells were harvested using trypsin and washed with PBS. The cells were fixed using 70% ethanol and stored at 4˚C for 48 hours. Next, the cells were stained with a solution containing 1 µg/ml RNase and 100 µg/ml PI and incubated at 37˚C for 30 minutes. Ultimately, the cell cycle of cancer cells was assessed using flow cytometry based on their fluorescence curve.

Statistical Analysis

In this investigation, all statistical analyses were conducted using Graph Pad Prism software version 8.1. Additionally, the two-way ANOVA method was employed to compare all data groups. The resulting statistics were presented as mean ± standard deviation. Significance thresholds for p-values were set at *<0.05, **<0.01, and ***<0.001. All experiments were performed in triplicate.

Results

Characterization of free niosome and cur-nio NPs

In recent years, niosomal nanocarriers have played an effective role in targeted therapy for cancer cells [21]. These nanoparticles can transport both hydrophobic and hydrophilic drugs [33]. The molecular biology activity of nanoparticles, such as niosome is largely influenced by their physicochemical properties [32]. PEGylation of nano-niosomes leads to improved stability, increased drug loading, reduced nanoparticle size, and modified drug release patterns [33]. Evaluating the physicochemical properties of nanoparticles, such as structure, size, zeta potential, and functional groups, is crucial for determining their medicinal applications [34]. The structure, functional groups, size, and surface charge of curcumin loaded in niosome nanoparticles were characterized using FE-SEM, FT-IR, DLS, and AFM methods [36, 37]. In 2014, a study presented findings on niosomal and liposomal systems containing paclitaxel. The drug efficiency in single and PEGylated vesicles was reported as 93% and 98%, respectively. Additionally, the efficiency of drug incorporation in free and PEGylated niosome was reported as 80% and 84%, respectively [38]. In this study, the synthesis of niosomal nanocarriers was conducted to determine their physicochemical properties. An optimal formulation was achieved with a molar ratio of 1:6 (cholesterol/surfactant) and an amount of 3.6 mg of curcumin. Also, the results of dynamic light scattering (DLS) showed that the size of the synthesized free niosome was 68.4±9.3 nm, and cur-nio was 98±17.5 nm. The polydispersity index (PDI) results for free niosome was 0.437, and for cur-nio was 0.503 (Table 2). The zeta potential of the blank niosome wss -8.49 ± 2.7, while that of the curcumin-loaded niosome was -11 ± 8.6 (Figure 3) and the entrapment efficiency of cur-nio was 85%.

The results of Fourier-transform infrared spectroscopy (FT-IR) showed that curcumin loaded in the niosome NPs. The spectra of blank niosome (Figure 4A) in the range of 3300-3600 cm-1 showed that it is assigned to O-H bonds of polymer. Also, the range of 1050-1150 proves the presence of an ether group in the niosome NPs structure. In free curcumin (Figure 4B), the range of 3200-3400 indicates the presence of alcohol group and the appearance

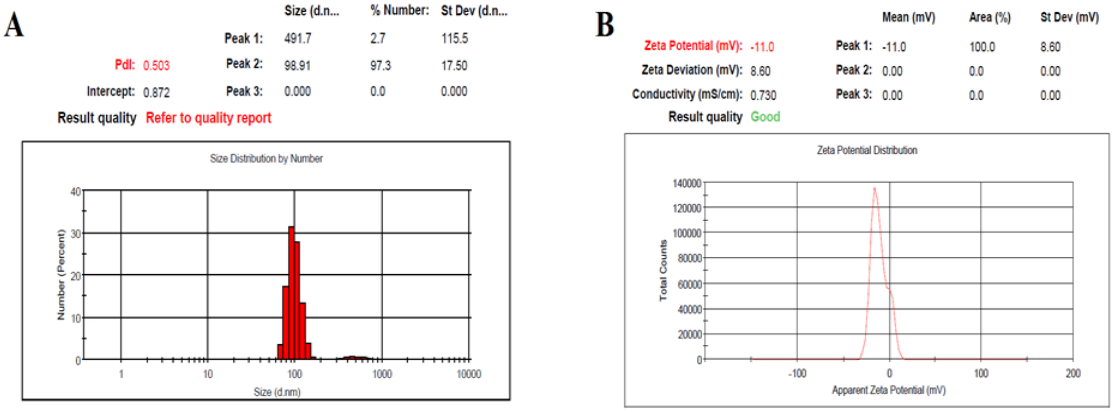

Figure 3. Dynamic Light Scattering (DLS) Characterization of Synthesized Nanoparticles. (A) The size and (B) zeta potential of curcumin-loaded niosomal nanoparticles (cur-nio). DLS results indicated that the size of cur-nio is larger than blank niosome, indicating effective loading of curcumin in the niosome.

Table 2. The Results of Size, PDI, and Zeta Potential of Blank Niosome and cur-Loaded Niosomal NPs.

Group	Size (nm)	Polydispersity(PDI)	Zeta potential (Mv)
Blank Niosome	68.4 ± 9.3	0.4370	-8.49 ± 2.7
Curcumin Loaded Niosome	98.9 ± 17.5	0.503	-11 ± 8.6

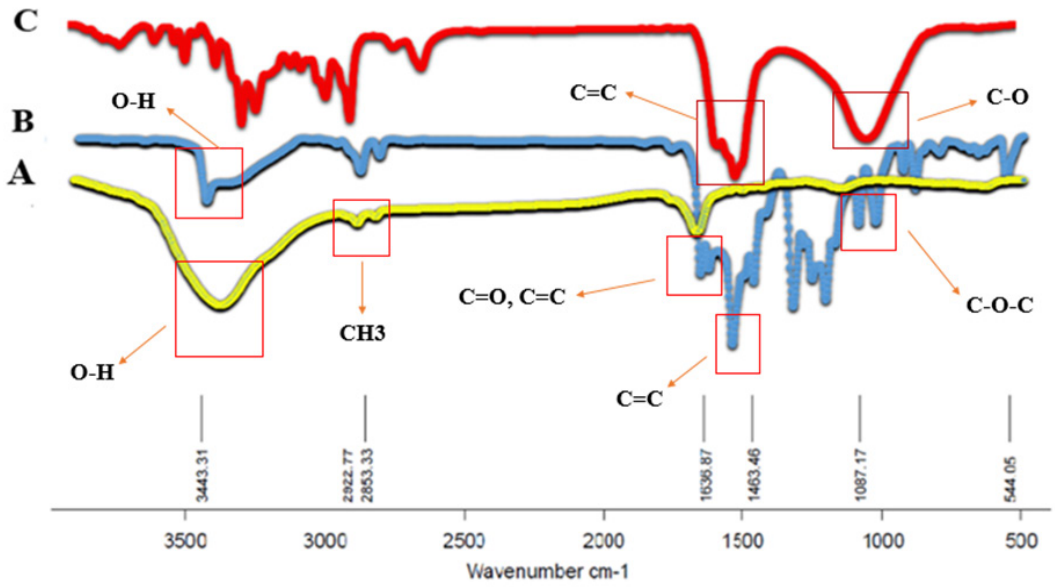

Figure 4. FT IR Spectra of Free nio, free Cur, and cur- nio NPs. Free niosome (A), free curcumin (B), and cur-nio NPs (C). The spectra of free niosome in the range of 3300-3600 cm-1 show O-H bonds. Also, the range of 1050-1150 is related to the presence of an ether group in free niosome. In free curcumin (B), the range of 3200-3400 indicates the presence of an alcohol group. Spectrum C indicates the presence of functional groups of curcumin and niosome, and it is inferred that curcumin is present inside niosome.

of the peak in the range of 1680 indicates the carbonyl group and 1200-1300 shows the presence of the phenolic group. In final spectrum (Figure 4C), a combination of both previous peaks has appeared, indicating the presence of curcumin inside the niosome NPs (Figure 4).

The atomic force microscopy (AFM) results indicate the topography of NPs. The results of AFM analysis illustrate that, the presence of particles with a height of approximately 82.2 nm from the surface is attributed to the curcumin-loaded niosome nanoparticles. This finding is consistent with the electron microscopic images of the samples and the estimated particle size (Figure 5).

The spherical and uniform shapes of curcumin loaded in niosome nanoparticles were observed using a Field Emission Scanning Electron Microscope (FE-SEM). The FE-SEM imaging of cur-nio revealed that these nanoparticles had smooth surfaces and homogeneous spherical shapes without aggregation. Also, no medicinal crystals were observed on the nanoparticles (Supplementary Figure 6).

Discussion

Drug release pattern

The release rate of curcumin-loaded niosome was investigated using a dialysis membrane at physiological pH (pH 7.4) and acidic pH (pH 5) for 100 hours at 37°C (Supplementary Figure 7). According to the results, the release of curcumin from niosome was performed in a biphasic profile. In the initial 24 hours, there was a burst release, with 80% released at acidic pH and 45% at physiological pH. This pattern remained stable for 5 days,

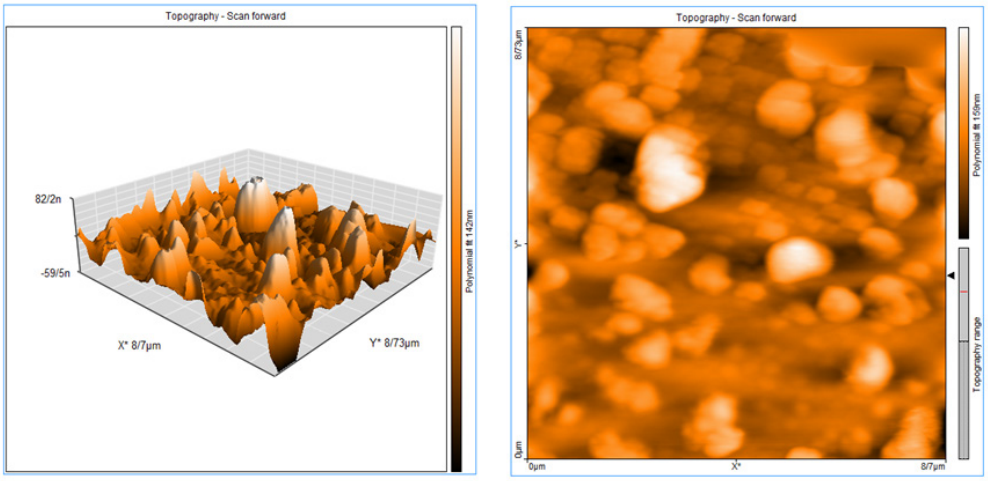

Figure 5. Atomic Force Microscopy (AFM) of Curcumin Loaded Niosome NPs.

with the maximum released curcumin reaching 90% in cancer conditions and 60% in physiological conditions. The possible cause for more release in the acidic condition of curcumin is the rapid degradation and hydrolysis of the polymer in the acidic environment [39]. The faster release of curcumin can be effective in the treatment of cancer in the acidic conditions [40]. It is a confirmed fact that the environment of cancer cells is acidic compared to blood and healthy cells [41]. In addition, cancer is associated with long-term treatment and different doses, so the controlled release of drugs from nano niosome during a long time is one of the attractions of this method [42, 43]. The hydrophobic polymer carriers have been implemented to deliver therapeutic molecules to the tumor location with controlled and slow release. In a study, Doxorubicin was entrapped in PGMD (poly-glycerol-malic acid-dodecanedioic acid) nanoparticles, and drug releasing process was monitored for 29 days. The release of Dox was 49% and 72% at physiological and acidic pH in the initial 5 hours [44]. In another study, which is about curcumin-loaded folate modified -chitosan nanoparticles, the release of curcumin was reported at pH=5 and pH=7. 4 around 90% and 75% for one week [45].

Cytotoxicity results

In the current study, the cytotoxic effect of free curcumin and curcumin-loaded niosome NPs with concentrations of 5, 10, 15, 20, 30, and 40 µM was investigated by MTT assay after 48 hours on the MDA-MB-231 breast cancer cell line. The results showed that the viability of cancer cells significantly decreased with the effect of free curcumin and cur-nio. Also, the effectiveness of cur-nio is higher than free cur. Based on the results, the IC_{50} value for cur-nio was 20 µM. Also, the IC_{50} for free curcumin was 30 µM (Supplementary Figure 8). This results demonstrates that the impact of cur-nio on cancer cells is greater than the free cur. In a study, the myristic acid-chitosan nano-formulation exhibited a higher cytotoxic effect compared to the curcumin nano-formulation [46]. In a similar study, it was observed that the cytotoxic effect of free curcumin decreased with prolonged incubation, while this effect increased in curcumin-loaded niosome nanoparticles after one week [47]. In 2018, a study was conducted on the encapsulation of Myrtus communis plant extract in a niosomal system and its effect on microbial pathogens. The results showed that the extract loaded in niosome with a lower inhibitory concentration demonstrated a better antimicrobial effect compared to the free form of the extract [48]. One of the mechanisms of the cytotoxic effects of the drug loaded in niosome is the combination of the niosome with the target cell membrane, which allows for the targeted delivery of the drug into the cell [49-51].

Gene expression analysis

Several studies have indicated that genetic mutations in the *RFC* gene can affect the absorption of folate [52]. Methotrexate is one of the chemotherapy drugs that enter the cell through *RFC* and inhibits folate pathway enzymes such as DHFR, but it shows drug resistance and gene mutation, and *RFC* does not allow it to enter [53]. Previous studies have shown that methylation of the *RFC* promoter, which reduces its expression, subsequently causes a disturbance in the absorption of methotrexate and its drug resistance in cancer cells [54]. According to these results, by increasing the expression of *RFC*, it is possible to intervene in the further absorption of methotrexate and then inhibit the folate pathway in cancer cells, thus contributing to the reduction of cancer cells [55]. Curcumin is a bioactive agent that inhibits the Topoisomerase enzyme of DNA synthesis [35]. This bioactive agent is an ideal option for stimulating apoptosis in breast cancer. Also, another study investigated the effect of Artemisia extract loaded in nisomes on the expression of the *BCL-2*/*BAX* gene in the MCF-7 cancer strain. Their research showed that the extract loaded in the noisome could increase *BAX* gene expression and decrease *BCL-2*. It indicates the induction of apoptosis in MCF-7 cells [56-58]. he present study exhibited a significant rise in *RFC* membrane protein and *BAX* gene expression compared to the control group in the MDA-MB-231 cells. In contrast, treatment of cells with cur-nio significantly decreased *BCL-2* expression. *RFC* and *BAX* gene expressions increase when treated with cur-nio, which has higher free curcumin (Supplementary Figure 9).

Apoptosis analyze

The Annexin V/PI staining method was used to understand the molecular basis of the inhibitory mechanism of cell growth caused by free cur and cur-nio. The results showed that the amount of apoptosis in MDA-MB-231 cells increased when exposed to free cur and cur-nio compared to the control group [59]. The findings indicate that the induction of apoptosis is done with high endocytosis in response to nano-formulation of curcumin [60-62]. According to previous findings, nano-formulation of bioactive compounds plays a significant role in preventing the proliferation of cancer cells and stimulating cell apoptosis [63, 64]. The results of this study presented that in Supplementary Figure 10A, which corresponds to the control group, 99% of MDA-MB-231 cells are viable while, in Supplementary Figure 10B, treated with free curcumin cells, 28% of cells are viable, 12% in early apoptosis. And 51% in late apoptosis and 8% in necrosis. In Supplementary Figure 10C, cells treated with cur-nio, 13% are alive, 17% are in the early apoptosis, 64% are in the late apoptosis stage, and 5% are necrosis. Therefore, based on the mentioned results, the apoptosis rate of MDA-MB-231 cells treated with curcumin-loaded noisome is higher than free curcumin (Supplementary Figure 10).

Cell cycle arrest

This test investigates the molecular mechanism of cell cycle and cell growth changes after exposure to blank curcumin and cur-nio nanoparticles [65]. In previous research, the results of stopping the cycle of cancer cells treated with curcumin and even as a combination of curcumin and chrysin were accumulated in the G2/M phase [66]. Also, previous studies indicated that curcumin loaded in nanoparticles could increase cell density in the sub-G1 phase by arresting the cell cycle in the G2/M phase

[67]. In addition, this operation related to cell cycle arrest in the G2/M phase has been shown in MDA cells in breast cancer [68]. The results of the current study are consistent with the studies of others. The present study found that curcumin loaded in niosome leads to high accumulation of cells in the sub-G1 phase. The nano delivery system is more effective than free curcumin in stopping the cell cycle in the G2/M phase and stimulating apoptosis. The treated MDA-MB-231 cells with curcumin loaded in niosome had above 30% accumulation of cells in the sub G1 phase by $p < 0.01$, while treatment of these cells with free curcumin caused less than 20% accumulation. The population of cells in the Sub-G1 phase indicates higher apoptosis of cancer cells treated with cur-nio compared to blank curcumin, which stops the cell cycle (Supplementary Figure 11).

In conclusion, in the present study, encapsulation of curcumin in niosome was characterized with DLS، FE-SEM، FT-IR, and AFM techniques. Furthermore, the cytotoxic impact of curcumin loaded in niosomes was greater than that of free curcumin, as evidenced by an IC_{50} value of 20 μM for these cells. The gene expression results indicate that the curcumin loaded in niosomes has led to an increase in the expression of *RFC* and *BAX* and a decrease in the expression of *BCL-2* in the MDA-MB-231 cancer cell line. Our results showed that the nano-formulation of bioactive compounds can serve as a complementary treatment alongside chemotherapy drugs like methotrexate. By using these compounds and overexpressing the *RFC* carrier, methotrexate can efficiently enter the cell and inhibit the target enzymes of the folate pathways, ultimately reducing the number of cancer cells. This study highlights the significance of the *RFC* gene in the treatment of breast cancer, which can be beneficial. Extensive studies can be conducted in vivo, including research on rats Supplementary Figure12.

Author Contribution Statement

Neda Iranpoor: Methodology, Investigation, Data curation, Original draft preparation. Davoud Jafari-gharabaghlou: Methodology, Investigation, Data curation, Original draft preparation. Siham Abdulzehra: Methodology, Investigation, Original draft preparation. Mohammad Reza Dashti: Reviewing and Editing.Fatemeh Ghorbanzadeh: Reviewing and Editing.Nosratollah Zarghami: Supervision, Conceptualization, Writing-Reviewing and Editing.

Acknowledgements

Availability of data and materials

The data and materials that support the findings of this study are available from the corresponding author, upon reasonable request.

Competing Interests

No potential competing interest was reported by the authors.

References

1. Sung H, Ferlay J, Siegel RL, Laversanne M, Soerjomataram I, Jemal A, et al. Global cancer statistics 2020: Globocan estimates of incidence and mortality worldwide for 36 cancers in 185 countries. CA Cancer J Clin. 2021;71(3):209-49. https://doi.org/10.3322/caac.21660.
2. Shepherd GM. Hypersensitivity reactions to chemotherapeutic drugs. Clin Rev Allergy Immunol. 2003;24(3):253-62. https://doi.org/10.1385/criai:24:3:253.
3. Peng Y, Nie J, Cheng W, Liu G, Zhu D, Zhang L, et al. A multifunctional nanoplatform for cancer chemo-photothermal synergistic therapy and overcoming multidrug resistance. Biomater Sci. 2018;6(5):1084-98. https://doi.org/10.1039/C7BM01206C.
4. Javan Maasomi Z, Pilehvar Soltanahmadi Y, Dadashpour M, Alipour S, Abolhasani S, Zarghami N. Synergistic anticancer effects of silibinin and chrysin in t47d breast cancer cells. Asian Pac J Cancer Prev. 2017;18(5):1283-7. https://doi.org/10.22034/apjcp.2017.18.5.1283.
5. Alibakhshi A, Ranjbari J, Pilehvar-Soltanahmadi Y, Nasiri M, Mollazade M, Zarghami N. An update on phytochemicals in molecular target therapy of cancer: Potential inhibitory effect on telomerase activity. Curr Med Chem. 2016;23(22):2380-93. https://doi.org/10.2174/0929867323666160425113705.
6. Ghanbari M, Saeedi M, Mortazavian AM. Nutraceuticals and functional foods production. Clinical-Excellence. 2016;5(1):1-15.
7. Firouzi-Amandi A, Tarahomi M, Rahmani-Youshanlouei H, Heris RM, Jafari-Gharabaghlou D, Zarghami N, et al. Development, characterization, and in vitro evaluation of cytotoxic activity of rutin loaded pcl-peg nanoparticles against skov3 ovarian cancer cell. Asian Pac J Cancer Preve. 2022;23(6):1951. https://doi.org/10.31557/APJCP.2022.23.6.1951
8. Shahbazi R, Jafari-Gharabaghlou D, Mirjafary Z, Saeidian H, Zarghami N. Design and optimization various formulations of pegylated niosomal nanoparticles loaded with phytochemical agents: Potential anti-cancer effects against human lung cancer cells. Pharmacol Rep. 2023;75(2):442-55. https://doi.org/10.1007/s43440-023-00462-8
9. Ghasemali S, Nejati-Koshki K, Akbarzadeh A, Tafsiri E, Zarghami N, Rahmati-Yamchi M, et al. Inhibitory effects of β-cyclodextrin-helenalin complexes on h-tert gene expression in the t47d breast cancer cell line-results of real time quantitative pcr. Asian Pac J Cancer Prev. 2013;14(11):6949-53. https://doi.org/10.7314/apjcp.2013.14.11.6949
10. Hatcher H, Planalp R, Cho J, Torti FM, Torti SV. Curcumin: From ancient medicine to current clinical trials. Cell Mol Life Sci. 2008;65(11):1631-52. https://doi.org/10.1007/s00018-008-7452-4.
11. Aggarwal BB, Harikumar KB. Potential therapeutic effects of curcumin, the anti-inflammatory agent, against neurodegenerative, cardiovascular, pulmonary, metabolic, autoimmune and neoplastic diseases. Int J Biochem Cell Biol. 2009;41(1):40-59. https://doi.org/10.1016/j.biocel.2008.06.010.
12. Sharma OP. Antioxidant activity of curcumin and related compounds. Biochem Pharmacol. 1976;25(15):1811-2. https://doi.org/10.1016/0006-2952(76)90421-4.
13. Esmaili M, Ghaffari SM, Moosavi-Movahedi Z, Atri MS, Sharifizadeh A, Farhadi M, et al. Beta casein-micelle as a nano vehicle for solubility enhancement of curcumin; food industry application. Lwt-Food Sci Technol. 2011;44(10):2166-72. https://doi.org/10.1016/j.lwt.2011.05.023.

14. Mohammadian F, Pilehvar-Soltanahmadi Y, Zarghami F, Akbarzadeh A, Zarghami N. Upregulation of mir-9 and let-7a by nanoencapsulated chrysin in gastric cancer cells. Artif Cells Nanomed Biotechnol. 2017;45(6):1201-6. https://doi.org/10.1080/21691401.2016.1216854
15. Rajiv J, Hardik J, Vaibhav S, Vimal A. Nanoburrs: A novel approach in the treatment of cardiovascular disease. Int Res J Pharm. 2011;2(5):91-2.
16. Steed JW, Turner DR, Wallace KJ. Core concepts in supramolecular chemistry and nanochemistry. John Wiley & Sons; 2007 Apr 30.
17. Pardakhty A, Moazeni E. Nano-niosomes in drug, vaccine and gene delivery: A rapid overview. Nanomed J. 2013;1(1):1-12. https://doi.org/10.22038/NMJ.2013.697
18. Mirahmadi N, Babaei MH, Vali AM, Dadashzadeh S. Effect of liposome size on peritoneal retention and organ distribution after intraperitoneal injection in mice. Int J Pharm. 2010;383(1-2):7-13. https://doi.org/10.1016/j.ijpharm.2009.08.034.
19. Kazi KM, Mandal AS, Biswas N, Guha A, Chatterjee S, Behera M, et al. Niosome: A future of targeted drug delivery systems. J Adv Pharm Technol Res. 2010;1(4):374-80. https://doi.org/10.4103/0110-5558.76435.
20. Rajera R, Nagpal K, Singh SK, Mishra DN. Niosomes: A controlled and novel drug delivery system. Biol Pharm Bull. 2011;34(7):945-53. https://doi.org/10.1248/bpb.34.945.
21. Kavussi HR, Miresmaeili SM, Lotfabadi NN. Niosomes from Preparation to Application in Drug Delivery. Journal of Shahid Sadoughi University of Medical Sciences. 2020. https://doi.org/10.18502/ssu.v28i2.3473.
22. Shilpa S, Srinivasan B, Chauhan M. Niosomes as vesicular carriers for delivery of proteins and biologicals. Int J Drug Deliv. 2011;3:14-24. https://doi.org/10.5138/ijdd.2010.0975.0215.03050.
23. Witika BA, Bassey KE, Demana PH, Siwe-Noundou X, Poka MS. Current advances in specialised niosomal drug delivery: Manufacture, characterization and drug delivery applications. Int J Mol Sci. 2022;23(17):9668. https://doi.org/10.3390/ijms23179668
24. Liu S, Wang ZM, Lv D-M, Zhao YX. Advances in highly active one-carbon metabolism in cancer diagnosis, treatment and drug resistance: A systematic review. Front Oncol. 2022;12. https://doi.org/10.3389/fonc.2022.1063305.
25. Sanchez H, Hossain MB, Lera L, Hirsch S, Albala C, Uauy R, et al. High levels of circulating folate concentrations are associated with DNA methylation of tumor suppressor and repair genes p16, mlh1, and mgmt in elderly chileans. Clin Epigenetics. 2017;9:74. https://doi.org/10.1186/s13148-017-0374-y.
26. Ma D, Huang H, Moscow JA. Down-regulation of reduced folate carrier gene (rfc1) expression after exposure to methotrexate in zr-75-1 breast cancer cells. Biochem Biophys Res Commun. 2000;279(3):891-7. https://doi.org/10.1006/bbrc.2000.4019.
27. Maddox DM, Manlapat A, Roon P, Prasad P, Ganapathy V, Smith SB. Reduced-folate carrier (rfc) is expressed in placenta and yolk sac, as well as in cells of the developing forebrain, hindbrain, neural tube, craniofacial region, eye, limb buds and heart. BMC Dev Biol. 2003;3:6. https://doi.org/10.1186/1471-213x-3-6.
28. Matherly LH, Hou Z, Deng Y. Human reduced folate carrier: Translation of basic biology to cancer etiology and therapy. Cancer Metastasis Rev. 2007;26(1):111-28. https://doi.org/10.1007/s10555-007-9046-2.
29. Al-Quteimat OM, Al-Badaineh MA. Practical issues with high dose methotrexate therapy. Saudi Pharm J. 2014;22(4):385-7. https://doi.org/10.1016/j.jsps.2014.03.002.
30. Nosrati H, Charmi J, Abhari F, Attari E, Bochani S, Johari B, et al. Improved synergic therapeutic effects of chemoradiation therapy with the aid of a co-drug-loaded nano-radiosensitizer under conventional-dose x-ray irradiation. Biomater Sci. 2020;8(15):4275-86. https://doi.org/10.1039/D0BM00353K.
31. Chancy CD, Kekuda R, Huang W, Prasad PD, Kuhnel JM, Sirotnak FM, et al. Expression and differential polarization of the reduced-folate transporter-1 and the folate receptor alpha in mammalian retinal pigment epithelium. J Biol Chem. 2000;275(27):20676-84. https://doi.org/10.1074/jbc.M002328200.
32. Frigerio B, Bizzoni C, Jansen G, Leamon CP, Peters GJ, Low PS, et al. Folate receptors and transporters: Biological role and diagnostic/therapeutic targets in cancer and other diseases. J Exp Clin Cancer Res. 2019;38(1):125. https://doi.org/10.1186/s13046-019-1123-1.
33. Eom YH, Kim HS, Lee A, Song BJ, Chae BJ. Bcl2 as a subtype-specific prognostic marker for breast cancer. J Breast Cancer. 2016;19(3):252-60. https://doi.org/10.4048/jbc.2016.19.3.252.
34. Azimian H, Dayyani M, Toossi MTB, Mahmoudi M. Bax/bcl-2 expression ratio in prediction of response to breast cancer radiotherapy. Iran J Basic Med Sci. 2018;21(3):325-32. https://doi.org/10.22038/ijbms.2018.26179.6429.
35. Choudhuri T, Pal S, Agwarwal ML, Das T, Sa G. Curcumin induces apoptosis in human breast cancer cells through p53-dependent bax induction. FEBS Lett. 2002;512(1):334-40. https://doi.org/https://doi.org/10.1016/S0014-5793(02)02292-5.
36. Mousazadeh N, Gharbavi M, Rashidzadeh H, Nosrati H, Danafar H, Johari B. Anticancer evaluation of methotrexate and curcumin-coencapsulated niosomes against colorectal cancer cell lines. Nanomedicine (Lond). 2022;17(4):201-17. https://doi.org/10.2217/nnm-2021-0334.
37. Zhao Z, Ukidve A, Krishnan V, Mitragotri S. Effect of physicochemical and surface properties on in vivo fate of drug nanocarriers. Adv Drug Deliv Rev. 2019;143:3-21. https://doi.org/10.1016/j.addr.2019.01.002.
38. Zare M, Arjmand M, Mohammadi M, Ebrahimi H, Akbarzadeh Ka. Preparation of Nanoniosomal Paclitaxel Formulation And Survey of it's (Cytotoxic Effect on Breast Cancer Cell Line Mcf-7). New Cellularand Molecular Biotechnology Journal. 2014;3(12):17-23
39. Gillies ER, Fréchet JMJ. Ph-responsive copolymer assemblies for controlled release of doxorubicin. Bioconjug Chem. 2005;16(2):361-8. https://doi.org/10.1021/bc049851c.
40. Ramasamy T, Tran TH, Choi JY, Cho HJ, Kim JH, Yong CS, et al. Layer-by-layer coated lipid-polymer hybrid nanoparticles designed for use in anticancer drug delivery. Carbohydr Polym. 2014;102:653-61. https://doi.org/10.1016/j.carbpol.2013.11.009.
41. Gillies RJ, Raghunand N, Karczmar GS, Bhujwalla ZM. Mri of the tumor microenvironment. J Magn Reson Imaging. 2002;16(4):430-50. https://doi.org/10.1002/jmri.10181.
42. Eisen SA, Miller DK, Woodward RS, Spitznagel E, Przybeck TR. The effect of prescribed daily dose frequency on patient medication compliance. Arch Intern Med. 1990;150(9):1881-4.
43. Salmani-Javan E, Jafari-Gharabaghlou D, Bonabi E, Zarghami N. Fabricating niosomal-peg nanoparticles co-loaded with metformin and silibinin for effective treatment of human lung cancer cells. Front Oncol. 2023;13:1193708. https://doi.org/10.3389/fonc.2023.1193708
44. Lei T, Manchanda R, Fernandez-Fernandez A, Huang YC, Wright D, McGoron AJ. Thermal and ph sensitive multifunctional polymer nanoparticles for cancer imaging

and therapy. RSC Adv. 2014;4(34):17959-68. https://doi.org/10.1039/c4ra01112k.
45. Esfandiarpour-Boroujeni S, Bagheri-Khoulenjani S, Mirzadeh H, Amanpour S. Fabrication and study of curcumin loaded nanoparticles based on folate-chitosan for breast cancer therapy application. Carbohydr Polym. 2017;168:14-21. https://doi.org/10.1016/j.carbpol.2017.03.031.
46. Khosropanah MH, Dinarvand A, Nezhadhosseini A, Haghighi A, Hashemi S, Nirouzad F, et al. Analysis of the antiproliferative effects of curcumin and nanocurcumin in mda-mb231 as a breast cancer cell line. Iran J Pharm Res. 2016;15(1):231-9.
47. Kumari M, Sharma N, Manchanda R, Gupta N, Syed A, Bahkali AH, et al. Pgmd/curcumin nanoparticles for the treatment of breast cancer. Sci Rep. 2021;11(1):3824. https://doi.org/10.1038/s41598-021-81701-x.
48. Raeiszadeh M, Pardakhty A, Sharififar F, Farsinejad A, Mehrabani M, Hosseini-Nave H, et al. Development, physicochemical characterization, and antimicrobial evaluation of niosomal myrtle essential oil. Res Pharm Sci. 2018;13(3):250-61. https://doi.org/10.4103/1735-5362.228955.
49. Abdelkader H, Alani AW, Alany RG. Recent advances in non-ionic surfactant vesicles (niosomes): Self-assembly, fabrication, characterization, drug delivery applications and limitations. Drug Deliv. 2014;21(2):87-100. https://doi.org/10.3109/10717544.2013.838077.
50. Abdulzehra S, Jafari-Gharabaghlou D, Zarghami N. Targeted delivery of oxaliplatin via folate-decorated niosomal nanoparticles potentiates resistance reversion of colon cancer cells. Heliyon. 2023;9(11):e21400. https://doi.org/10.1016/j.heliyon.2023.e21400
51. Ghorbanzadeh F, Jafari-Gharabaghlou D, Dashti MR, Hashemi M, Zarghami N. Advanced nano-therapeutic delivery of metformin: Potential anti-cancer effect against human colon cancer cells through inhibition of gpr75 expression. Med Oncol. 2023;40(9):255. https://doi.org/10.1007/s12032-023-02120-8
52. Gong M, Yess J, Connolly T, Ivy SP, Ohnuma T, Cowan KH, et al. Molecular mechanism of antifolate transport-deficiency in a methotrexate-resistant molt-3 human leukemia cell line. Blood. 1997;89(7):2494-9.
53. Matherly LH, Hou Z. Structure and function of the reduced folate carrier a paradigm of a major facilitator superfamily mammalian nutrient transporter. Vitam Horm. 2008;79:145-84. https://doi.org/10.1016/s0083-6729(08)00405-6.
54. Li WW, Takahashi N, Jhanwar S, Cordon-Cardo C, Elisseyeff Y, Jimeno J, et al. Sensitivity of soft tissue sarcoma cell lines to chemotherapeutic agents: Identification of ecteinascidin-743 as a potent cytotoxic agent. Clin Cancer Res. 2001;7(9):2908-11.
55. Worm J, Kirkin AF, Dzhandzhugazyan KN, Guldberg P. Methylation-dependent silencing of the reduced folate carrier gene in inherently methotrexate-resistant human breast cancer cells. J Biol Chem. 2001;276(43):39990-40000. https://doi.org/10.1074/jbc.M103181200.
56. Dabaghian Amiri A, Mirzaie A, Ali Asgari E, Mahmoudzadeh A. Preparation of niosome loaded Artemisia chamamelifolia extract: antibacterial and anti-cancer activities and apoptosis gene expression analysis in breast cancer cell line (MCF-7). Feyz Medical Sciences Journal. 2021 Mar 10;25(2):839-49.
57. Mohammadinejad S, Jafari-Gharabaghlou D, Zarghami N. Development of pegylated plga nanoparticles co-loaded with bioactive compounds: Potential anticancer effect on breast cancer cell lines. Asian Pac J Cancer Prev. 2022;23(12):4063. https://doi.org/10.31557/APJCP.2022.23.12.4063
58. Amirsaadat S, Jafari-Gharabaghlou D, Dadashpour M, Zarghami N. Potential anti-proliferative effect of nano-formulated curcumin through modulating micro rna-132, cyclin d1, and htert genes expression in breast cancer cell lines. J Clust Sci. 2023;34(5):2537-46.
59. Faramarzi L, Dadashpour M, Sadeghzadeh H, Mahdavi M, Zarghami N. Enhanced anti-proliferative and pro-apoptotic effects of metformin encapsulated plga-peg nanoparticles on skov3 human ovarian carcinoma cells. Artif Cells Nanomed Biotechnol. 2019;47(1):737-46. https://doi.org/10.1080/21691401.2019.1573737.
60. Farajzadeh R, Pilehvar Y, Dadashpour M, Javidfar S, Lotfi-Attari J, Sadeghzadeh H, et al. Nano-encapsulated metformin-curcumin in plga/peg inhibits synergistically growth and htert gene expression in human breast cancer cells. Artif Cells Nanomed Biotechnol. 2017;46:1-9. https://doi.org/10.1080/21691401.2017.1347879.
61. Cai X, Hu X, Tan X, Cheng W, Wang Q, Chen X, et al. Metformin induced ampk activation, g0/g1 phase cell cycle arrest and the inhibition of growth of esophageal squamous cell carcinomas in vitro and in vivo. PLoS One. 2015;10(7):e0133349. https://doi.org/10.1371/journal.pone.0133349.
62. Jafari-Gharabaghlou D, Pilehvar-Soltanahmadi Y, Dadashpour M, Mota A, Vafajouy-Jamshidi S, Faramarzi L, et al. Combination of metformin and phenformin synergistically inhibits proliferation and htert expression in human breast cancer cells. Iran J Basic Med Sci. 2018;21(11):1167. https://doi.org/10.22038/IJBMS.2018.30460.7345
63. Xie W, Wang L, Sheng H, Qiu J, Zhang D, Zhang L, et al. Metformin induces growth inhibition and cell cycle arrest by upregulating microrna34a in renal cancer cells. Med Sci Monit. 2017;23:29-37. https://doi.org/10.12659/msm.898710.
64. Jafari-Gharabaghlou D, Dadashpour M, Khanghah OJ, Salmani-Javan E, Zarghami N. Potentiation of folate-functionalized plga-peg nanoparticles loaded with metformin for the treatment of breast cancer: Possible clinical application. Mol Biol Rep. 2023;50(4):3023-33. https://doi.org/10.1007/s11033-022-08171-w
65. Javan N, Khadem Ansari MH, Dadashpour M, Khojastehfard M, Bastami M, Rahmati-Yamchi M, et al. Synergistic antiproliferative effects of co-nanoencapsulated curcumin and chrysin on mda-mb-231 breast cancer cells through upregulating mir-132 and mir-502c. Nutr Cancer. 2019;71(7):1201-13. https://doi.org/10.1080/01635581.2019.1599968.
66. Hu S, Xu Y, Meng L, Huang L, Sun H. Curcumin inhibits proliferation and promotes apoptosis of breast cancer cells. Exp Ther Med. 2018;16(2):1266-72. https://doi.org/10.3892/etm.2018.6345.
67. Mayol L, Serri C, Menale C, Crispi S, Piccolo MT, Mita L, et al. Curcumin loaded plga-poloxamer blend nanoparticles induce cell cycle arrest in mesothelioma cells. Eur J Pharm Biopharm. 2015;93:37-45. https://doi.org/10.1016/j.ejpb.2015.03.005.
68. Lv ZD, Liu XP, Zhao WJ, Dong Q, Li FN, Wang HB, et al. Curcumin induces apoptosis in breast cancer cells and inhibits tumor growth in vitro and in vivo. Int J Clin Exp Pathol. 2014;7(6):2818-24.